

Study on energy saving of cross-ventilated detached house using coupling techniques of network model and semi-empirical ventilation model

M. Ohba, K. Tsukamoto

*Wind Engineering Research Center, Tokyo Polytechnic University, Tokyo, 243-0297 Japan
(Corresponding author: Email: ohba@arch.t-kougei.ac.jp)*

ABSTRACT: A semi-empirical ventilation model (LDSM) based on local dynamic similarity theory was coupled with COMIS and TRNSYS. The COMIS-LDSM model provided us with valuable information on inflow/outflow angles at openings. The accuracy of the ventilation flow rate prediction was increased by 5% to 20% compared to the orifice model with fixed discharge coefficients. A simulation study on cooling load was performed in a detached house. The cooling load was reduced by 17% by opening windows when a room was occupied and by 58% by opening windows whenever possible compared with the cooling load when all windows remained closed.

KEY WORDS: Cross-ventilation, Energy Saving, Cooling load, Network model, Local dynamic similarity model

1 INTRODUCTION

It is important to utilize natural energy such as cross-ventilation to create comfortable living spaces. It should be possible to increase ventilation flow rates by devising ways of opening windows to create the best paths for cross-ventilation and by keeping windows open for longer periods. This in turn will reduce air-conditioner cooling loads. An orifice model assuming constant discharge coefficients regardless of wind directions is widely used to predict ventilation flow rates. However, discharge coefficients vary greatly according to wind direction and opening location. To solve this problem, the authors proposed an empirical model based on results of research on CFD analysis and of wind tunnel experiments. The empirical model, called a Local Dynamic Similarity Model (LDSM), expresses the variation of discharge coefficient with wind direction [1]. The LDSM can predict ventilation flow rates more accurately than the conventional method [2].

This paper describes the newly developed COMIS-LDSM model where COMIS is used as a network model for ventilation simulation. The LDSM was applied to inflow/outflow openings of COMIS code [3]. Then, the effects of reducing cooling loads through cross-ventilation for a detached house was evaluated by coupled simulation on the COMIS-LDSM and a thermal and multi-zone model (TRNSYS).

2 OUTLINE OF THE COMIS-LDSM MODEL

2.1 Local Dynamic Similarity Model (LDSM)

Figure 1 shows the pressure balance in the vicinity of an inflow opening. The pressure field at the inflow opening can be represented by three pressures: dynamic pressure normal to the opening (P_n), dynamic pressure tangential to the opening (P_t) and ventilation driving pressure (P_r). Thus, total pressure P_T at an inflow opening is $P_n + P_t + P_s$.

The local dynamic similarity model assumes that P_n , which is directly related to ventilation flow rate (Q), is uniquely determined by P_t and P_r , and that there are dynamic similarities in the relationships among the three pressures when the ratios of P_r to P_t are coincident and determined by Formula (1), as shown in Table 1. The discharge coefficient (C_d) and the inflow angle (β) are described by the ratios of P_n to P_r and P_t to P_n , which are determined by Formula (2) and Formula (3), respectively. The characteristics of ventilation performance through an opening can be represented by Formulae (6) and (7). Appropriate discharge coefficients can be calculated from Formulae (1) to (7) even when wind direction angles and opening locations are different.

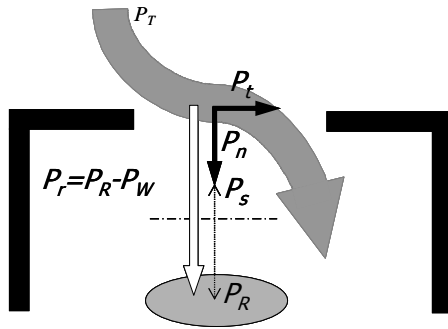


Figure 1. Dynamic similarity in vicinity of inflow opening

Table 1. Fundamental formulas of local dynamic similarity model

$$P_R^* = \frac{P_r}{P_t} \quad (1) \quad C_d = \sqrt{\frac{P_n}{|P_r|}} \quad (2)$$

$$\beta = \tan^{-1} \sqrt{\frac{P_t}{P_n}} \quad (3) \quad P_r = P_R - P_W \quad (4)$$

$$Q = C_d A \sqrt{\frac{2}{\rho} |P_r|} \quad (5)$$

$$C_d = C_{ds} \left(\frac{P_R^*}{P_{RS}^*} \right)^n \quad (|P_R^*| \leq |P_{RS}^*|) \quad (6)$$

$$C_d = C_{ds} \quad (|P_R^*| \geq |P_{RS}^*|) \quad (7)$$

2.2 COMIS-LDSM model

Figure 2 outlines the COMIS-LDSM model [3]. The COMIS code was revised on the basis of LDSM model to calculate the discharge coefficients and airflow rates at inflow/outflow openings. P_W and P_t for the building envelope are provided as input data. The ventilation performances of inflow/outflow openings are also provided as input data. Arbitrary room pressure (P_R) is given as an initial condition and a discharge coefficient corresponding to P_R^* is selected from the ventilation performance curve. The calculation was performed by the Relaxation-Newton method until ventilation flow rates of outflow and inflow in each room were balanced.

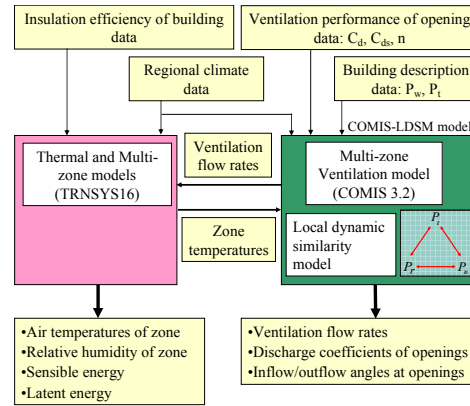


Figure 2. Block diagram of COMIS-LDSM & TRNSYS model

3 REVIEW ON PREDICTION ACCURACY OF VENTILATION FLOW RATES WITH USING COMIS-LDSM MODEL

3.1 Outline of wind tunnel experiments

In order to verify the validity of the coupled model, wind tunnel experiments were conducted in an Eiffel-type wind tunnel (1,200mm wide by 1,000mm high) at Tokyo Polytechnic University [3]. The building model had two rooms with openings 40mm wide by 20mm high, as shown in Figure 3. The opening in the partition wall was located at the center to reduce the effect of the inflow dynamic pressure on the outflow. The outflow opening was located at the side wall of the leeward room. The direction of the approach flow was varied in the range of -22.5° to 67.5° . The approach flow was a boundary layer flow with a power-law index of 0.25, and the reference velocity was kept at 7.0m/s at the upwind edge of the model.

Figure 4 shows the ventilation performance for inflow/outflow openings. For a wind angle of -22.5° , the approach flow directly affected the airflow characteristics at the outflow opening so that the static pressure along the outflow greatly changed. For the outflow opening at a wind angle of -22.5° we used different parameters from the prescribed ones. We set C_{ds} to 0.79, P_{RS}^* to 0.67, and n to 0.61. The C_d of the opening in the partition wall was set to a constant value of 0.63.

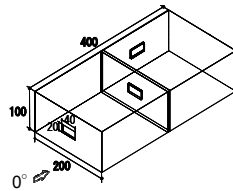


Figure 3. Cross-ventilation model

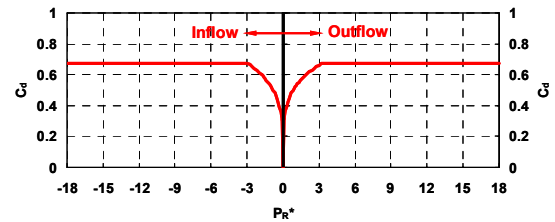


Figure 4. Ventilation performance expressions for inflow and outflow openings

3.2 Results of prediction accuracy of discharge coefficients and ventilation flow rates

Figure 5 indicates the measured and predicted discharge coefficients. The experimental values of

C_d were calculated from the measured ventilation flow rates, room pressures and wind pressures. The conventional orifice model used a C_d of 0.67 for both inflow and outflow openings, regardless of wind angle. The experimental discharge coefficients were not fixed, but varied depending on wind direction. The COMIS-LDSM model had almost the same discharge coefficients as the experimental ones at the inflow opening. Even at the outflow opening, the predicted discharge coefficients followed the trend of the experimental discharge coefficients.

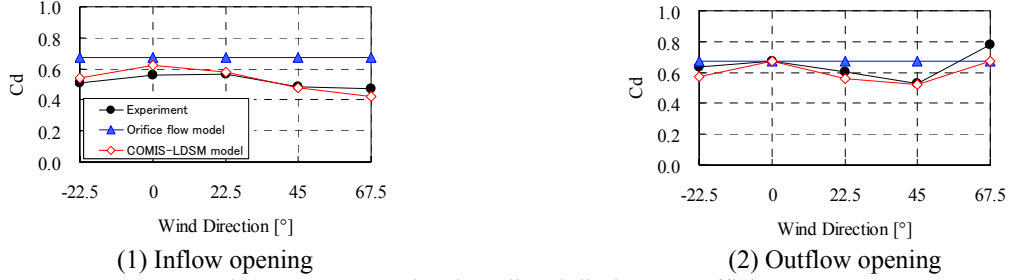


Figure 5. Measured and predicted discharge coefficients

As shown in Figure 6, the COMIS-LDSM indicated better predictions for all wind angles than the conventional orifice model. The prediction accuracy increased by 5% to 20% compared to the orifice model. The conventional orifice model cannot predict the ventilation flow rate accurately because the interfering cross-flow dynamic pressure P_t is too high at either inflow opening or outflow opening when the wind direction is not normal to the openings.

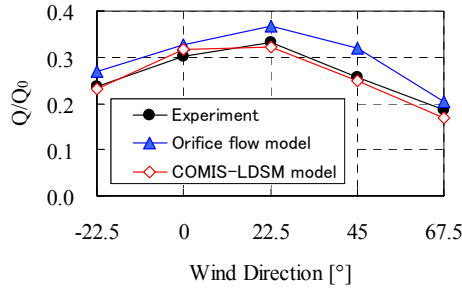


Figure 6. Measured and predicted ventilation flow rates

4 SIMULATION STUDY ON EFFECTS OF REDUCING COOLING LOADS THROUGH CROSS-VENTILATION IN DETACHED HOUSE

4.1 Simulation outline

This simulation study was performed for a typically shaped residential house defined by the Architectural Institute of Japan (AIJ) to calculate the cooling load reduction effect when utilizing cross-ventilation [4,5]. As shown in Figure 7, the family in the studied house was assumed to be composed of four persons: two children, a daily commuter and a homemaker. It had 2 stories and a total floor area of 120 m², comprising six rooms including a living room kitchen. The eave height was 5.4m. It was also assumed that the house was located in the suburbs with no other buildings around it and it was insulated according to next-generation energy standards. Windows in habitable rooms and halls, and room doors were opened and closed according to the logic of opening/closing windows and the logic of turning on/off air-

conditioners. Windows and doors in the toilets, bathroom and washrooms were kept closed. The inside and outside temperature was set to 20°C, assuming that there was no buoyancy-driven ventilation.

The expanded AMEDAS weather data were used for the meteorological data in Tokyo and the period was set to the month of June. The wind profile had a power index of 0.32. The ventilation performance of the outside windows was as shown in Figure 4. The discharge coefficients of the room doors were set to 0.63. P_w and P_t of the wall openings and roof window were obtained beforehand from a 1/40 scale model through a wind tunnel experiment.

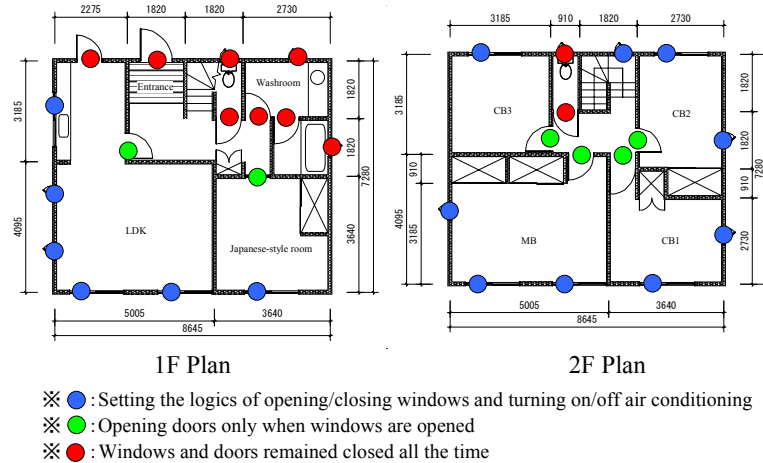


Figure 7. Plan of AIJ residential model

4.2 Logic of opening/closing windows and turning on/off air-conditioner

The decision tree of operation of cooling and windows is shown in Figure 8 [6]. The logic of turning on/off air-conditioners was applied to only the LDK, the master bedroom and the two children's rooms. Air-conditioners were not used in the other rooms. When the room temperature exceeded 28°C in an occupied room, the air-conditioner was turned on and when the room temperature dropped below 27°C, the air-conditioner was turned off. The cooling temperature controlled by the air-conditioners was set to 28°C and the humidity to 60%. The logic of opening/closing windows was applied to the windows and doors in the habitable rooms and the hall.

Three cases were simulated. For Case 1, we only used the logic of turning on/off air-conditioners with all windows closed. For Case 2, the basic logic of opening/closing windows was used. Windows were opened in occupied rooms when the temperature exceeded 24°C and closed when the temperature dropped below 23°C. Windows were closed when all family members would be sleeping or when rooms were not occupied. For Case 3, the active logic of opening/closing doors was used. When the house was occupied (even when residents were asleep or the rooms were not occupied), we opened the windows 20% when the room temperature exceeded 24°C and closed them when the temperature dropped below 23°C. Doors in habitable rooms were opened when the windows were opened and the doors were closed when the air-conditioners were on and/or the windows were closed.

The schedule of persons at home was followed according to Table 2 proposed by AIJ. The same pattern was used during weekdays and weekends. It was assumed that nobody occupied the house from 14:00-16:00 and the family was asleep from 23:00-6:00. It was also assumed that

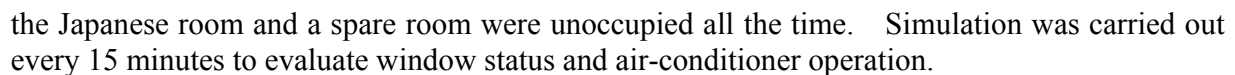


Figure 8. Operation of cooling and window

Table 2. Schedule of occupied time zone

	1	2	3	4	5	6	7	8	9	10	11	12	13	14	15	16	17	18	19	20	21	22	23	24
LDK							1	4	1	1	1	1	1	1			3	3	3	3	2	2	1	
MB	2	2	2	2	2	2	1																1	2
CB1	1	1	1	1	1	1	1													1	1	1	1	1
CB2	1	1	1	1	1	1	1														1	1	1	1

4.3 Simulation results for cooling loads in LDK for a single day

Figure 9 shows room window operation, air-conditioner operation and room temperature in the LDK. The average meteorological data of June 18 were used. In Case 1, where the doors were not closed or opened routinely, air-conditioners were turned on when the rooms were occupied from 6:00-14:00 and from 16:00-23:00. The temperature rose to 30°C from 14:00-16:00 on the unoccupied time zone. The room temperature exceeded 26°C even while residents were sleeping. The room temperature was 4°C to 6°C higher than the outside temperature and the fluctuation of room temperature was minor throughout the day.

In Case 2, the windows were opened from 6:00-14:00 and the room temperature tended to be slightly higher than the outside temperature. Because the windows were closed from 23:00-6:00, room temperature was 2°C to 5°C higher than the outside temperature.

In Case 3, the windows were closed from 6:00-14:00 and room temperature showed almost the same tendency as the outside temperature. Because the windows were opened 20% even while residents were asleep from 23:00-6:00, changes in room temperature had the same tendency as the outside temperature. The room temperature in Case 3 was 3°C to 4°C lower than in Case 1 and 2°C lower than in Case 2 except when the air-conditioners were turned on, so the operating time of the air-conditioners could be reduced.

Figure 10 indicates the cooling load history in the LDK for a day. In Case 1, the air-conditioners were operated from 6:00-14:00, so cooling load was generated. However, because cross-ventilation was working during those hours in Case 2 and Case 3, there was no cooling load. Because the air-conditioners were operated from 16:00-23:00 pm in all cases, cooling loads were generated. However, cooling loads in Case 3 were slightly smaller than in Case 2 because the room temperature in Case 3 was lower than the room temperature in Case 2.

Figure 11 shows the number of air exchanges in the LDK. Because the windows were opened 20% even while residents were asleep from 23:00-6:00 in Case 3, the number of air exchanges was about 20 per hour. In Case 3, the windows in the habitable rooms other than the LDK were

also opened 20% from 6:00-14:00, so the number of air exchanges increased by about five per hour compared with Case 2.

The schedule of persons at home was followed according to Table 2 proposed by AIJ. The same pattern was used during weekdays and weekends. It was assumed that nobody occupied the house from 14:00-16:00 and the family was asleep from 23:00-6:00. It was also assumed that the Japanese room and a spare room were unoccupied all the time. Simulation was carried out every 15 minutes to evaluate window status and air-conditioner operation.

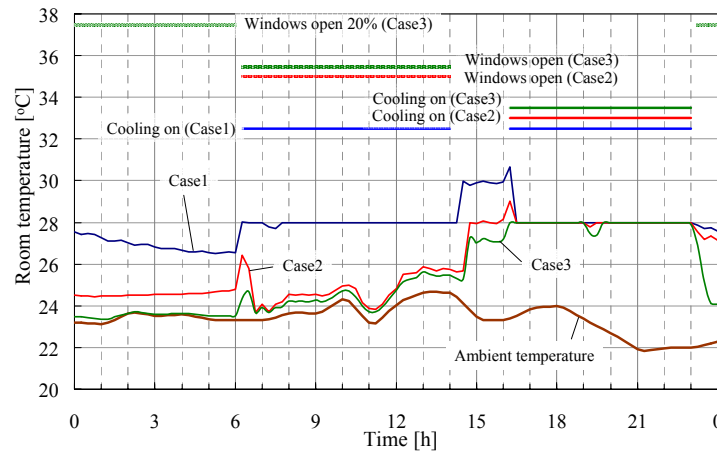


Figure 9. Time-history of room temperatures in LDK for a day

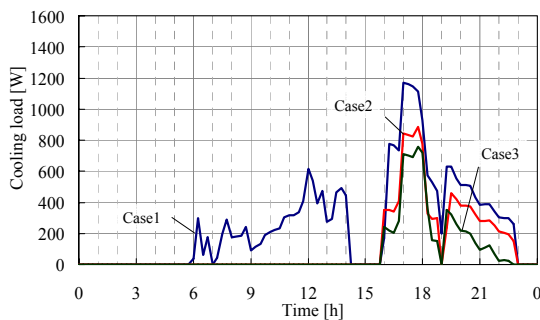


Figure 10. Time-history of cooling loads in LDK

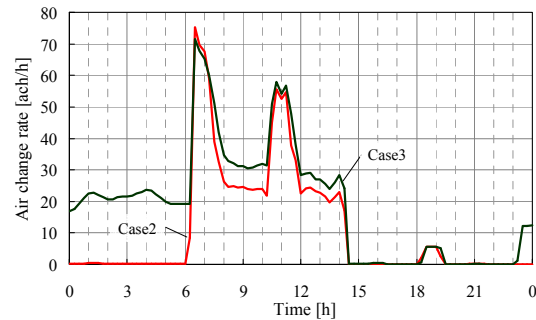


Figure 11. Time-history of air exchange rates in LDK

4.4 Simulation results for cumulative cooling loads in LDK for the month of June

Figure 12 compares the duration of the operating time of the air-conditioners in June. Reduction of air-conditioner operating time of 98 hours was achieved for the LDK, and of 8 to 26 hours for other habitable rooms by opening the windows during the occupied time zone in Case 2 versus Case 1. In Case 3, where the windows were opened liberally at night, further reduction of air-conditioner operating time of 120 hours was achieved in the LDK and the air-conditioners did not need to be operated in the other habitable rooms.

Figure 13 compares the cumulative time the windows remained open. The cumulative time the windows remained fully open was longest in the LDK, and shortest in the master bedroom in both Case 2 and Case 3. However, if the length of time the windows remained 20% open is included, the length of time windows remained open in the master bedroom and the children's rooms exceeded 350 hours in Case 3, over 120 hours longer than in the LDK. Opening the windows 20% greatly helped the utilization of cross-ventilation.

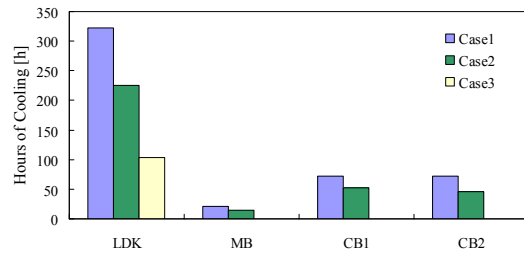


Figure 12. Cumulative operating hours of air conditioners in June

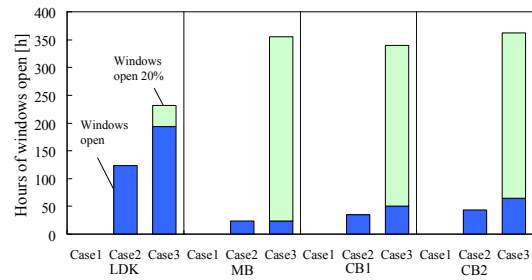


Figure 13. Cumulative hours during which windows remained open in June

Table 3 shows the cumulative cooling loads in June and the effects of reducing energy through cross-ventilation in Cases 1, 2 and 3. Utilization of cross-ventilation succeeded in reducing cooling loads by 45 KW (17%) compared to those required when the windows were closed. In addition, when the windows also remained open during the unoccupied time zone or while residents were sleeping, the cooling load was 152 KW less than that required when the windows remained closed. It was 99 KW less than the cooling load required when the windows remained open in the occupied rooms. The cooling load was reduced by 58% compared to that when all windows remained closed.

Table 3. Cumulative cooling load and its reduction ratio by cross-ventilation

Case	Window operation	Cumulative Cooling load [KW]	Reduction of cooling load [%]
1	Closed	264	—
2	Basic Opened/Closed	219	17.0
3	Active Opened/Closed	112	57.6

5 CONCLUSION

A semi-empirical ventilation model based on local dynamic similarity theory was coupled with COMIS and TRNSYS, which are widely used for energy conservation simulation. The COMIS-LDSM model provided us with valuable information on inflow/outflow angles at openings. It is very useful for predicting flow patterns in rooms. The prediction accuracy of ventilation flow rates was increased by 5% to 20% compared with the orifice model using fixed discharge coefficients.

A simulation study was performed on cooling loads in a detached house. We succeeded in reducing the cooling load by 17% by opening windows when a room was occupied and by 58% by opening windows whenever possible compared with the cooling load when all the windows remained closed.

ACKNOWLEDGEMENTS

This study was partially funded by the Ministry of Education, Culture, Sports, Science and Technology, Japan, through the Global Center of Excellence Program of Tokyo Polytechnic University.

REFERENCES

1. Kurabuchi T, Ohba M, Endo T et al. (2004). Local dynamic similarity of cross-ventilation, Part 1 Theoretical framework, *International Journal of Ventilation*, Vol.2, No 1, pp.371-382.
2. Ohba M, Goto T, Kurabuchi T et al. (2006). Experimental study on predicting wind-driven cross-ventilation flow rates and discharge coefficients based on the Local dynamic similarity model, *International Journal of Ventilation*, Vol.5, No 1, pp.105-114.
3. Ohba M, Kurabuchi T, Goto T et al. (2008). Prediction accuracy of ventilation flow rates by COMIS model combined with local dynamic similarity model, *Annual meeting of AIJ*, pp.753-754.
4. Udagawa H (1985). Typical problems for house, 15th Heat Symposium.
5. Ohba M, Kurabuchi T, Goto T et al. (2008). Study on prediction of ventilation flow rates in detached house based on coupled simulation of semi-empirical envelope flow model and network model, *Proceedings of 4th International Conference on Advances in Wind & Structures*, pp.1156-1166.
6. Nagai T (2006). Windows and HVAC operation to reduce cooling requirement by means of cross-ventilation, *International Journal of Ventilation*, Vol.5, No 1, pp.151-162.

Study on thermal comfort in quasi-cross-ventilated environment using climate chamber

M. Ohba, K. Mizutani, K. Tsukamoto¹

¹*Wind Engineering Research Center, Tokyo Polytechnic University, Tokyo, 243-0297 Japan
(Corresponding author: Email: ohba@arch.t-kougei.ac.jp)*

ABSTRACT: We adopted a hot environment condition with the temperature set to 35°C and the relative humidity set to 70% in a newly constructed climate chamber, and investigated the excreted sweat and the skin surface temperature on different parts of the human body in relation to steady wind at various mean velocities. There were considerable individual differences in the relationship between the amounts of sweat produced at different parts of the body and at different wind velocities. However, the amount of sweat produced generally decreased as wind velocity increased.

KEY WORDS: Climate Chamber, Cross-Ventilated Environment, Thermal Comfort, Steady Flow

1 INTRODUCTION

The effective use of natural cross-ventilation is being studied with a view to improving indoor thermal environments using natural energies. The authors conducted an experiment using human subjects in an actual housing space. It was found that natural crosswind fluctuated in direction and velocity with lower frequency than that generated by an electric fan or an air conditioner, and hence natural crosswind could produce a more cooling breeze effect. We were unable, however, to study the relationship between natural crosswind fluctuations and environmental factors such as the cooling effect of sweat evaporation. This was mainly because it was difficult to maintain the exact same environmental conditions for different subjects when conducting the experiment [1].

In this study, a climate chamber was constructed to enable us to systematically analyze the relationship between natural crosswind fluctuations, the amount of sweat produced, and the skin temperature. We investigated the excreted sweat and the skin surface temperature on different parts of the human body in relation to steady wind at various mean velocities.

2 OVERVIEW OF CLIMATE CHAMBER

Figure 1 shows a plan view of the climate chamber and Figure 2 shows the interior of the laboratory inside the climate chamber. The climate chamber was designed to meet the following air-conditioning requirements:

* Temperature: 20 to 35°C \pm 0.5°C

- * Humidity: 40 to 70% \pm 2%
- * Wind velocity: 0.1 to 2.0 m/s

The climate chamber is 5 m wide \times about 11 m long \times about 3 m high. It houses a laboratory 3.7 m wide \times 8 m long \times 2.7 m high, a pre-room, and a fan room.

The climate chamber is equipped with:

- * a heat source system consisting of a hot-water boiler and a brine chiller unit;
- * two compact air-conditioning units (one with an air supply capacity of 3,000 m³/h and a cooling and heating capacity of 10.5 KW, and the other with an air supply capacity of 2,000 m³/h and a cooling and heating capacity of 7.0 KW); and
- * an electrically-heated vaporizing humidifier (10.0 Kg/h).

Figure 3 shows the airflow generator installed in the fan room. It is comprised of 48 plug fans driven by 280-W DC motors. We planned to reproduce the long-frequency fluctuations of the natural crosswind by controlling the revolution speeds of each motor from a desktop computer.

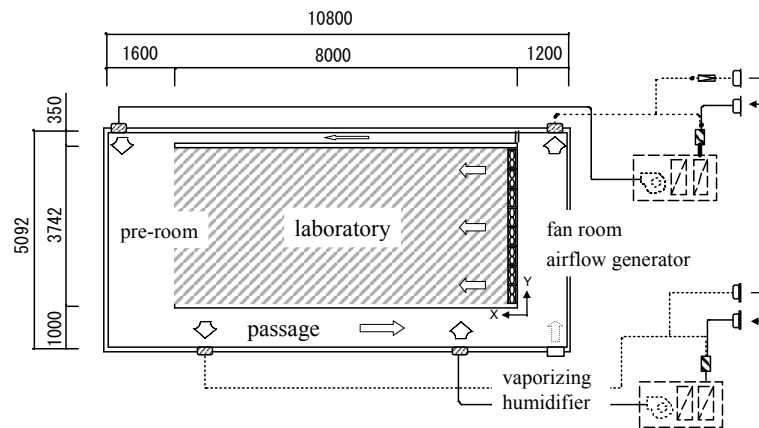


Figure 1. Plan view of Climate Chamber



Figure 2. Interior of laboratory inside climate chamber



Figure 3. Fan room

3 OVERVIEW OF EXPERIMENT ON SUBJECTS

Table 1 shows the experimental conditions. With the room temperature and relative humidity in the climate chamber fixed to 35°C and 70%, respectively, the wind velocity was changed to 0.1, 0.45, 0.98, and 1.5 m/s so that the physical conditions of each subject could be measured under four different experimental conditions. The duration of the experiment was 60 minutes. Eight young male students were selected as subjects of the study, and asked to wear a designated pair of

trunks. General information regarding these subjects is shown in Table 2. Characteristics regarding the amount of sweat produced were compiled based on subjective responses given by the subjects in a questionnaire.

Table 1. Experimental conditions.

Case No	Environmental condition				condition of human body		number of subject
	wind velocity [m/s]	air temperature [°C]	MRT [°C]	relative humidity [%]	metabolic rate [met]	Clothing [clo]	
1	0.10	34.9	35.5	68.2	1.46	0.03	8
2	0.45	34.9	35.4	69.7	1.38	0.03	8
3	0.98	35.1	35.8	68.5	1.48	0.03	8
4	1.50	35.1	35.9	68.4	1.51	0.03	8

Table 2. General information regarding human subjects

subject	height [cm]	weight [kg]	surface area [m ²]	body sensitivity	sweat level
a	172.6	66.6	1.74	neutral	little
b	158.0	55.1	1.51	cold	much
c	184.7	70.9	1.87	hot	very much
d	167.7	57.2	1.60	neutral	slightly much
e	173.9	61.1	1.68	hot	much
f	167.1	64.7	1.68	hot	very much
g	167.6	59.2	1.62	cold	little
h	165.3	68.8	1.60	hot	very much

4 RELATIONSHIP BETWEEN AMOUNT OF SWEAT PRODUCED AND WIND VELOCITY

Sweating is an essential means of releasing heat when humans are in a hot environment. In the experiment, amounts of sweat excreted from various parts of each subject's body were measured, and the relationship between amount of sweat and wind velocity was analyzed.

Figure 4 shows how the amount of sweat produced by subject "d" changed with time when the wind velocity was set to 0.45 m/s. The perspiration meter had two measurement channels (1 and 2) and could take two measurements simultaneously. Thus, channel 1 was used continuously and exclusively to measure the amount of sweat produced on the forehead while channel 2 was assigned to measure the amount of sweat produced at six other parts of the body of each subject: chest, back, belly, femoral region, leg region and insteps. Each part was measured for ten minutes so the measurement of all six parts was completed in 60 minutes. The amount of sweat produced on the forehead was approximately 0.9 mg/min, which was greater than that produced at other parts of the body, and this fluctuated over a cycle of two to five minutes. Differences between the amounts of sweat produced at different parts of the body were noted. For example, a large amount of sweat was produced on the chest and back, while only a little was found on the hands and insteps.

Figure 5 shows how the weight of subject "h" changed with time when the wind velocity was set to 0.1 m/s. A gradual decrease in weight with subject was noted. The subject weighed 220 g less at the end of the experiment than at the start. This loss of weight by the subject is equivalent to the total evaporation through sweat and through expiration. The amount of sweat produced by

the whole body included the amount of evaporation through sweat and the amount of drips of sweat that adhere to the underwear and the skin. Therefore, the loss of weight by the subject, the increase in the weight of the trunks, and the increase in weight of a towel that absorbed sweat dripping from the subject or adhering to the skin were totaled, and the resulting value was defined as the amount of sweat produced by the whole body.

Figure 6 shows the relationship between the amount of sweat produced by the whole body and the amount of evaporation from the whole body. Individual differences in the amount of sweat produced by the whole body were relatively small; the amount of sweat produced by the whole body of each subject was in the range of 0.11 to 0.33 mg/min/cm². We noted that when the wind velocity was low so that the amount of sweat produced by the whole body increased to more than 0.2 mg/min/cm², the difference between the amount of sweat produced by the whole body and the amount of evaporation from the whole body became large. Consequently, the rate at which sweat evaporated (evaporation rate) decreased.

Figure 7 shows the relationship between the mean amounts of sweat produced by and evaporation from the whole body of each subject and the wind velocities. The amount of sweat produced by the whole body was about 0.16 mg/min/cm² and this was hardly affected by change in the wind velocity. On the other hand, the amount of evaporation from the whole body decreased when the wind velocity decreased; the evaporation rate reduced to around 80% at a wind velocity of 0.1 m/s, while it was 95% at a wind velocity of 1.5 m/s.

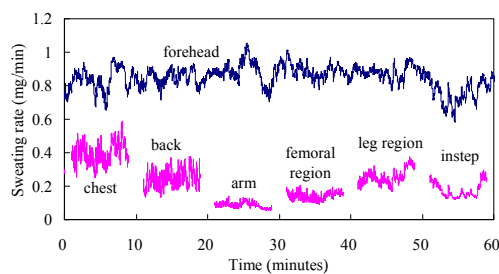


Figure 4. Time history of sweat rate for subject (d) for 0.45 m/s

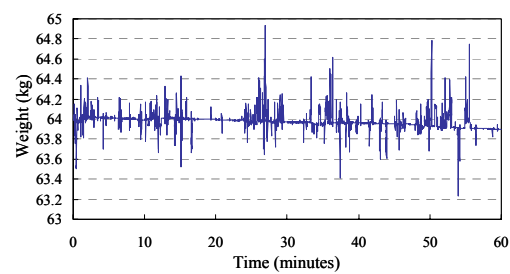


Figure 5. Time history of weight for subject (h) for 0.1 m/s

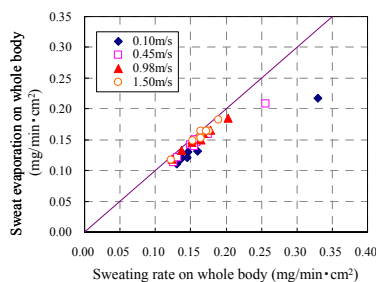


Figure 6. Relationship between sweat rate and evaporation rates excreted from whole bodies

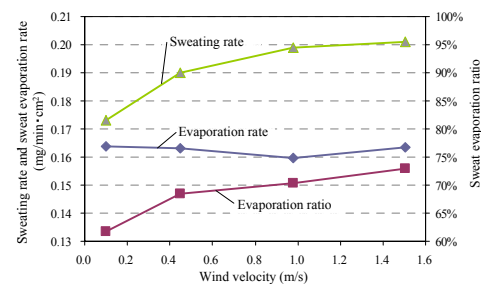


Figure 7. Relationship among sweat rate & evaporation rates excreted from whole bodies and different wind velocities

5 RELATIONSHIP BETWEEN SKIN-SURFACE TEMPERATURE AND WIND VELOCITY

How the skin-surface temperatures of the subjects varied with wind velocity was investigated with consideration given to the amount of thermal sweating. The setup of the experiment is shown in Figure 8. In previous studies, the mean skin-surface temperature (t_{sk}) was calculated

based on the heat balance on the body surface by considering conditions such as the degree of sweating and the proportion of clothing that was wet. In this study, the mean skin-surface temperature was calculated by using Equation (1) below, in which the body part area ratio proposed by Hardy-DuBois was used for weighting [2].

$$tsk = 0.07 \times \text{forehead} + 0.35 \times (\text{chest} + \text{back}) / 2 + 0.07 \times \text{upper arms} + 0.07 \times \text{forearms} + 0.05 \times \text{backs of the hands} + 0.19 (\text{femoral region 1} + \text{femoral region 2}) / 2 + 0.2 \times \text{lower legs} [^{\circ}\text{C}] \quad (1)$$

Figure 9 shows the mean values for the inner ear temperatures (deep temperatures) and the skin temperatures of each subject measured at four different wind velocities during the 60-minute period. The inner ear temperatures remained almost constant at around 37°C , and individual differences in these temperatures were as small as about 0.5°C . The average skin temperatures, however, ranged from 34°C , where sweating begins, to 36°C . This indicates that the rate of thermal sweating for the whole body increases in proportion to the mean skin temperature. While there were considerable variations in the skin temperatures of the subjects in an environment in which the wind velocity was high, there was little variation when the wind velocity was low. When the wind velocity was high, some subjects had low skin temperatures while others had high skin temperatures, and the individual differences were 1°C or more.

Figure 10 shows the mean skin temperatures at each part of the body of eight subjects at each wind velocity. In the environment where there were strong air streams, there were considerable variations in skin temperatures at different parts of the body. The difference between the skin temperature at various parts of the body were about 1°C when the temperature was 34°C in some



Figure 8. Human subject

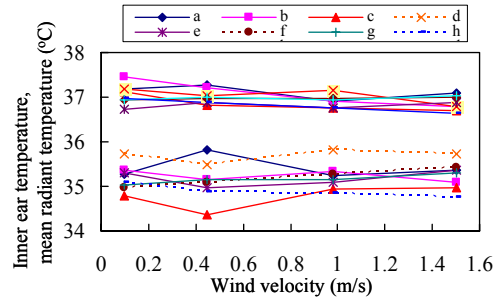


Figure 9. Inner ear temperature and skin surface temperature for different velocities

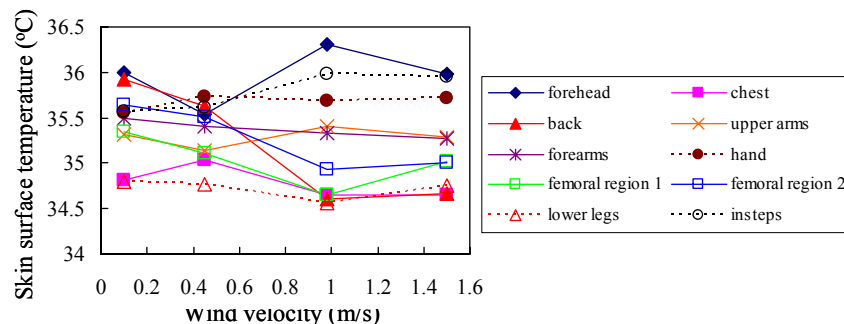


Figure 10 Mean skin temperatures at different parts of the body of eight subjects at different wind velocities.

cases, where the air streams were considered calm using the Hardy-DuBois technique. In this experiment, however, they were somewhat larger, between 1.7 and 2.1°C, because higher wind velocities were used. While the skin temperature of the forehead was highest and those of the hands and insteps were also high, the skin temperatures of the chest, the lower legs, and femoral region 1 (near the lower leg), which were directly exposed to blowing air, were low. This reveals that the skin temperatures were high at parts of the body with a small surface area, exposed to air streams, or at parts of the body where the heat flow transpiration rate or transpiration rate was low due to lower wind velocities. On the other hand, it was low at parts of the body directly exposed to air streams when the wind velocity was high. In addition, the skin temperature on the back of the body, with wind velocity of 0.1 or 0.45 m/s, was lower than that with wind velocity of 1.0 or 1.5 m/s. This is thought to be because as the wind velocity increased, the air streams flowed to the back, thereby causing the transpiration rate to increase.

6 CONCLUSION

We obtained the following findings from this experiment, which was conducted using human subjects in a hot environment with a temperature set to 35°C and a relative humidity set to 70%:

- 1) Although there were considerable individual differences in the relationship between the amount of sweat produced at each part of the body and the wind velocity, the general tendency was for the amount of sweat produced to decrease as the wind velocity increased.
- 2) Individual differences in the amount of sweat produced by the whole body were smaller compared with individual differences in the amount of sweating at each part of the body. In addition, the effect of wind velocity on the amount of sweating on the body as a whole was minimal.
- 3) The amount of evaporation from the whole body changed with wind velocity and the evaporation rate decreased as the wind velocity decreased.
- 4) Although the mean skin-surface temperature was minimally affected by wind velocity, the skin temperatures at different parts of the body were considerably affected by the area exposed to the air streams and the directions of the air streams.
- 5) Individual differences in the amount of sweat produced were closely associated with individual differences in the mean skin temperature.

ACKNOWLEDGEMENTS

This study is partly supported by the Grant-in-Aid for Scientific Research (B) of JSPS (20360265). This study was also partially funded by the Ministry of Education, Culture, Sports, Science and Technology, Japan, through the Global Center of Excellence Program of Tokyo Polytechnic University.

REFERENCES

1. Yukari Iino, Masaaki Ohba, Akinaru Iino and Tetsuo Annaka: STUDY ON EVALUATIONS OF THERMAL ENVIRONMENT UNDER CROSS VENTILATION AND AIRFLOWS FROM AIR-CONDITIONING SYSTEM AND ELECTRIC FAN, Proceedings of Indoor Air Quality, Ventilation and Energy Conservation in Buildings (IAQVEC), 2007.10
2. Ken Parsons, Human Thermal Environments Second edition, CRC Press

Development of a natural ventilation system with constant air volume during velocity fluctuations

K. Mizutani¹

¹*Wind Engineering Research Center, Tokyo Polytechnic University, Tokyo, 243-0297 Japan
(Corresponding author: Email: mizutani@arch.t-kougei.ac.jp)*

ABSTRACT: We improved backdraft dampers based on the experiments, and reviewed the conditions for obtaining constant air volume characteristics with the use of weights and springs. As a result, we succeeded in developing natural ventilation dampers that keep a constant air volume under conditions ranging from low to high wind pressure.

KEY WORDS: Natural ventilation system, Constant air volume, backdraft damper

1 INTRODUCTION

Rooms need ventilation as long as they are occupied, and much energy is consumed for many hours at a time in offices and stores. In addition, because 24-hour ventilation is now required for housing, constant ventilation needs to be secured like in offices. However, reliance on air-conditioning equipment will increase running costs, so a natural ventilation system which runs cheaply and can also contribute to energy saving is now attracting attention. Natural ventilation can be provided at a low cost and requires less energy. However, because an unstable natural wind is utilized, the amount of ventilation varies a lot depending on the wind conditions. Because of this, there is a demand for a natural ventilation system that can take in a uniform amount of air regardless of whether the wind blows weakly or strongly.

It is for this reason that we conducted this research, resulting in the development of a natural ventilation system with constant air volume which provides stable ventilation with an unstable natural wind.

2 THEORETICAL STUDY ON A NATURAL VENTILATION SYSTEM WITH CONSTANT AIR VOLUME

2.1 *Natural ventilation systems*

Consistently maintaining uniform ventilation has been difficult because a changing natural force is utilized to achieve natural ventilation. However, it is believed that the amount of ventilation can be controlled, regardless of the magnitude of wind pressure, by using a damper that reduces the area of the ventilation opening when wind pressure increases (see Figure 1).

2.2 Use of backdraft dampers

A backdraft damper is usually used so a damper spring (hereafter called a “spring”) opens when a fan sends out air, and closes to prevent backflow when the fan stops. However, it is possible to provide an opening with a spring that closes when the wind increases by using a backdraft damper that can open fully when there is no wind. So, a backdraft damper should be used with the wind coming from the outside so the spring closes when a strong wind blows, and it opens when a weak wind blows. Figure 2 shows how the backdraft damper can be used.

2.3 Obtaining a constant air volume

If the backdraft damper is used only as shown in Figure 2, the spring stops abruptly when wind pressure suddenly increases. The result is that ventilation cannot be stable. So, it is necessary to exercise ingenuity in devising a spring that exerts a force opposite of the wind pressure so that it opens when a weak wind blows, and closes gradually when a strong wind blows.

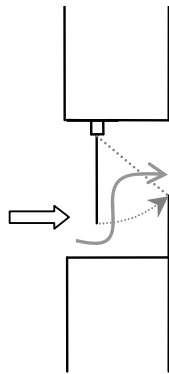


Figure 1: Proposed damper

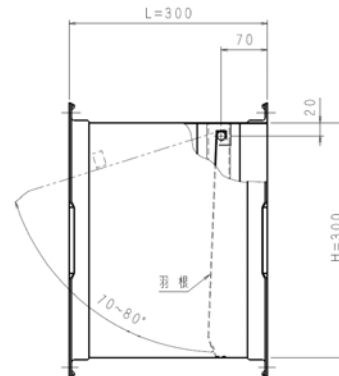


Figure 2: Use of a backdraft damper

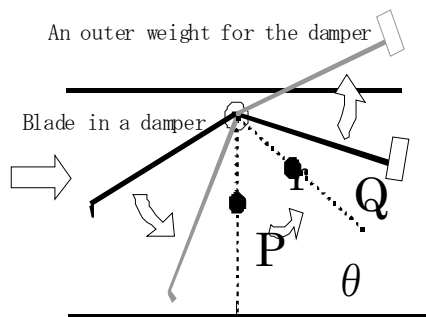


Figure 3: Concept of the backdraft damper



Photo 1: Improved backdraft damper

2.4 Improvement of backdraft dampers with the use of springs and weights

We used springs and weights to make a backdraft damper that can provide a constant volume of air. With the location of a weight adjusted for a backdraft damper as shown in Figure 3, a vane can open fully when there is no wind. At this time, the total center of gravity of the vane and weight outside the backdraft damper is located right under the shaft of the vane (at point P). If the wind blows in such a situation, the wind hits the vane, and the force of the wind generates power to push the vane. If the vane pushed by the wind force rotates θ degrees, the weight will rise and the total center of gravity will move θ degrees from point P (to point Q). As a result, the vane stops at a point where the power and the wind force are balanced because of the generated restoring force (a clockwise rotary force) that can be found using the formula $(mg \sin\theta \times r)$ with the radius of the center of gravity as r (m).

However, because the rise in restoring force caused by the displaced center of gravity is smaller than the rise in wind force, it can be assumed that the vane will immediately close completely when a strong wind blows, and the amount of ventilation will decrease considerably. Therefore, we came up with a shape that would increase the rotation angle of the vane and increase the restoring force by using a spring as well (Photo 1).

Let's take a look at a situation with a spring located as shown in Figure 4. When the wind force is small, the stretch of the spring is small because the movement of the vane is small. However, the stretch of the spring (from point A to point O, and from point B to point O) increased when wind force gradually increased (Figure 5). Because the restoring force of the spring increases in proportion to the stretch of the spring, we believe that a phenomenon where the vane closes completely when a strong wind blows can be avoided. Therefore, we conducted experiments concerning the characteristics of the velocity of the damper with different springs and weights.

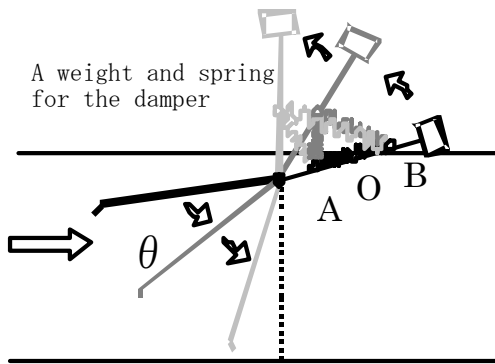


Figure 4: Damper with a spring

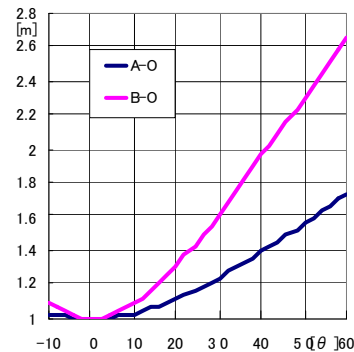


Figure 5: Length and angle of the spring



Photo 2: Laboratory device for Case 1 to Case 9



Photo 3: Laboratory devices for Case 10

3 OUTLINE OF EXPERIMENTS


3.1 Experiments

Table 1 outlines the experiments. We conducted experiments for a total of 10 configurations. For Case 1 to Case 9, we used weights, and changed the number and location of springs. For Case 10, we used a ready-made product. For each case, we obtained the characteristics of Point P and Point Q in the damper by changing the rotations per minute of a fan with an inverter in order to change the pressure difference in front of and behind the damper, and measure velocity at that time with a wind gauge.

Table 1: Conditions for experiments 1 to 10

	Weight	Between “A” and “O”	Between “B” and “O”	Remarks
Case 1	○			
Case 2	○	A damper vane was fixed.		
Case 3	○	a		
Case 4	○	b		
Case 5	○	b	a	
Case 6	○	a	b	
Case 7	○	b	c	Photo 4
Case 8	○	b	c	
Case 9	○		c	Photo 5
Case 10	A ready-made constant air volume damper for natural ventilation was used.			

Table 2: Size of spring (mm)

Spring	a	b	c
Wire diameter	1.0	0.9	0.65
Outer diameter	13.5	8	8
Total length	62.5	70	50
Photo of external appearance			

3.2 Laboratory devices

Photo 2 shows a laboratory device. The section of a duct measures 300 mm by 300 mm, and the total length of the duct is 2,240 mm. A backdraft damper was installed at a location 1,000 mm away from a fan. To measure the difference in pressure in front of and behind the damper, we used a differential pressure gauge, and installed a wind gauge at the exit of the duct (wind exit). For Case 10, we changed the shape of the duct to conduct the experiment because we used a ready-made product as a natural ventilation system. Photo 3 shows the laboratory devices for this experiment.

4 EXPERIMENT RESULTS

Case 1 to Case 10: Figure 6 (a pressure difference of up to 300 Pa) and Figure 7 (a pressure difference of up to 30 Pa) indicate the relationship between the pressure difference in front of and behind the damper, and velocity in Case 1 to Case 10.

Case 1: We conducted an experiment with a weight and no spring. As the rotations per minute of the fan increased, the pressure difference in front of and behind the damper increased, as did the velocity. With a pressure difference of 5 Pa, the velocity was about 600 m³/h. After that, the damper started to close gradually, and the increase of velocity slowed down. After the velocity exceeded 800 m³/h with a pressure difference of 25 Pa, velocity did not increase even though the pressure difference increased. With a pressure difference of more than 150 Pa, the damper closed completely, and velocity lowered to about 300 m³/h.

Case 2: We fixed the damper at an intermediate position. As a result, velocity became proportional to the inverse square of the pressure difference. Velocity was less than Case 1 with a pressure difference of up to 50 Pa, but velocity was more than Case 1 with a pressure difference of more than 50 Pa. We concluded that a constant air volume was not maintained.

Case 3: We used a spring to prevent the damper from suddenly closing completely as seen in Case 1. As a result, with a pressure difference of more than 150 Pa, we were able to maintain a velocity of about 800 m³/h. However, velocity increased gradually with a pressure difference of up to 30 Pa (within a range of a pressure difference at a general velocity), and it was hoped that the characteristics of a constant volume of air would be maintained within the range of a smaller pressure difference.

Case 4: Spring a used in Case 3 was replaced with Spring b. As a result, the amount of ventilation started to be stabilized at a slightly earlier stage compared to Case 3, but it was about the same as Case 1. And there was no significant difference when compared within a pressure difference range of up to 30 Pa.

Case 5: Based on the results of Cases 3 and 4, we provided spring b between “A” and “O,” and spring a between “B” and “O,” and changed the location of the weight. As a result, we were able to obtain 1,000 m³/h or more ventilation when the pressure difference was small, and the amount of ventilation with a pressure difference of 20 Pa or more either stabilized or decreased. However, because ordinary wind pressure around buildings is usually 20 Pa or less, it was hoped that the amount of ventilation would be stabilized when a weak wind blows with a smaller pressure difference.

Case 6: We interchanged the spring between “A” and “O” and the spring between “B” and “O” used in Case 5, and conducted an experiment for comparison. As a result, the volume of air

with a pressure difference of 20 Pa or more did not change, but the amount of ventilation decreased slightly when a weak wind with a minor pressure difference blew.

Case 7: In order to stabilize the amount of ventilation when a weak wind blows, we replaced the spring between “B” and “O” with spring c so that the spring would start to close with a small pressure difference, and close with difficulty under a larger pressure. In addition, we moved the weight upward in order to move the center of gravity of the system closer to the axis of rotation, and to create a system operated only by the power of the springs, not by the weight (Photo 4). Consequently, the amount of ventilation was almost stabilized with a pressure difference of 5 Pa or more. However, with a larger pressure difference, vibration was generated tending toward a loss of stability.

Case 8: In order to maintain stability with a certain amount of ventilation secured during weak wind conditions, we improved Case 7, in consideration of the relationship between the stretch of the springs and the restoring force, and the center of gravity, by fine-tuning the location of each. As a result, we were able to obtain a stable amount of ventilation with a pressure difference of 9 Pa or more without vibration.

Case 9: As a result of applying values obtained in Case 8 to actual meteorological data, we found it was necessary to maintain a certain amount of ventilation with a lower pressure difference because the amount of ventilation did not stabilize during weak wind conditions. Because of this, we fine-tuned the system based on previous data so that the amount of ventilation could be stabilized during weak wind conditions, and so that the spring could move with a single spring even during weak wind conditions (Photo 5). Consequently, we succeeded in maintaining a certain amount of ventilation (500 m³/h) with a pressure difference of 2 Pa during weak wind conditions.

Case 10: We took a measurement using a commercially available constant air volume damper for natural ventilation. We found that the amount of ventilation was almost stabilized at 1,000 m³/h with a pressure difference of 40 Pa to 150 Pa, and that the amount of ventilation could not be stabilized with a pressure difference of under 30 Pa.



Photo 4: Case 7



Photo 5: Case 9

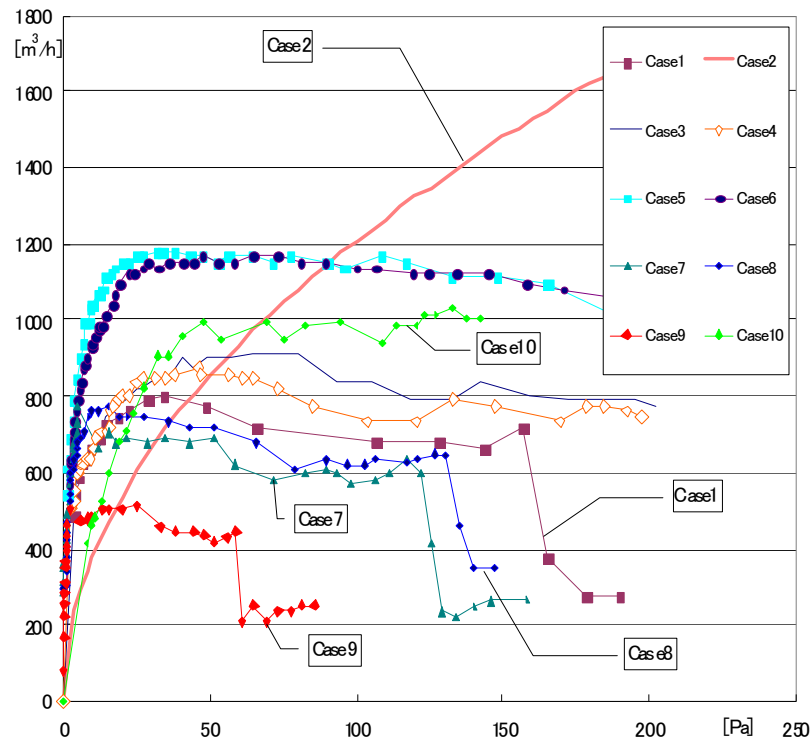


Figure 6: Relationship between the pressure difference in front of and behind a damper, and an air volume (1)

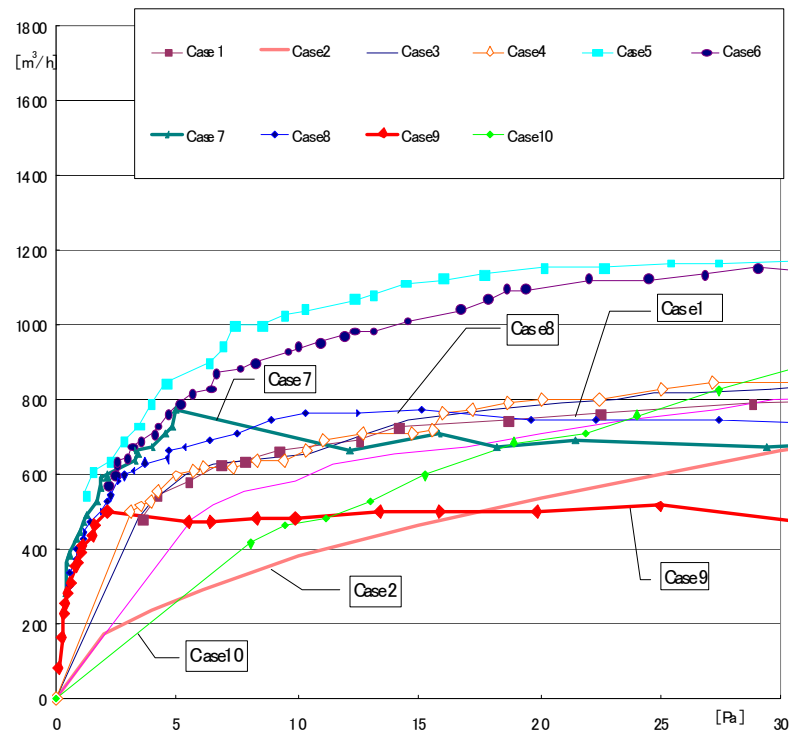


Figure 7: Relationship between the pressure difference in front of and behind a damper, and an air volume (2)

5 CONCLUSION

We improved backdraft dampers based on the experiments, and reviewed the conditions for obtaining constant air volume characteristics with the use of weights and springs.

As a result, we succeeded in developing natural ventilation dampers that keep a constant air volume under conditions ranging from low to high wind pressure.